Spectroscopic Signatures of Halogens in Clathrate Hydrate Cages. 1. Bromine

Galina Kerenskaya,* Ilya U. Goldschleger, V. Ara Apkarian, and Kenneth C. Janda

Department of Chemistry, University of California Irvine, Irvine, California 92697

Received: July 17, 2006; In Final Form: October 19, 2006

We report the first UV−vis spectroscopic study of bromine molecules confined in clathrate hydrate cages. Bromine in its natural hydrate occupies $5^{12}6^2$ and $5^{12}6^3$ lattice cavities. Bromine also can be encapsulated into the larger $5^{12}6^4$ cages of a type II hydrate formed mainly from tetrahydrofuran or dichloromethane and water. The visible spectra of the enclathrated halogen molecule retain the spectral envelope of the gas-phase spectra while shifting to the blue. In contrast, spectra of bromine in liquid water or amorphous ice are broadened and significantly more blue-shifted. The absorption bands shift by about 360 cm^{-1} for bromine in large $5^{12}6^4$ cages of type II clathrate, by about 900 cm^{-1} for bromine in a combination of $5^{12}6^2$ and $5^{12}6^3$ cages of pure bromine hydrate, and by more than 1700 cm^{-1} for bromine in liquid water or amorphous ice. The dramatic shift and broadening in water and ice is due to the strong interaction of the water lone-pair orbitals with the halogen σ^* orbital. In the clathrate hydrates, the oxygen lone-pair orbitals are all involved in the hydrogen-bonded water lattice and are thus unavailable to interact with the halogen guest molecule. The blue shifts observed in the clathrate hydrate cages are related to the spatial constraints on the halogen excited states by the cage walls.

Introduction

Although the halogen clathrate hydrates have been known for nearly 200 years, we have not been able to locate any optical spectroscopic studies of these species. This is rather surprising since spectroscopy is often the first tool of choice for studying bonding and intermolecular interactions. Chlorine hydrate, the earliest gas clathrate hydrate discovered, was first prepared by Davy in 1811;[1] bromine hydrate was prepared about 20 years later.[2] The stoichiometry and structure of these clathrate hydrates were quite controversial until those of chlorine hydrate were conclusively determined by X-ray crystallography.[3] It was found that the water lattice is formed from two types of cages, denoted 5^{12} and $5^{12}6^2$. The 5^{12} cages are dodecahedra of 20 water molecules with 12 pentagonal faces, as shown in Figure 1. The $5^{12}6^2$ cages are made from 24 water molecules with 12 pentagonal faces and two hexagonal faces. To achieve three-dimensional packing, the crystal has three $5^{12}6^2$ cages for every 5^{12} cage. Such a clathrate hydrate structure is called "type I". In a perfect crystal with complete cage filling by chlorine, the overall stoichiometry of the unit cell would be $(Cl_2)_8(H_2O)_{46}$. However, the small cages are usually not fully occupied, and therefore the chlorine-to-water ratio is typically somewhat smaller.[4]

The structure of bromine clathrate hydrate is considerably more complicated than that of chlorine clathrate hydrate. The stoichiometry is variable enough that, although the correct unit cell was first determined in 1963,[5] it was later postulated that there are several different stable structures.[6] In 1997, Ripmeester et al.[7] determined that a single structure accounts for all stable cage-filling ratios. The crystal consists of three types of cages, 5^{12}, $5^{12}6^2$, and $5^{12}6^3$, in a 10:16:4 ratio. In a perfect clathrate crystal, bromine molecules would occupy the $5^{12}6^2$ and $5^{12}6^3$ cages, but not the 5^{12} cages, for an overall unit cell stoichiometry of $(Br_2)_{20}(H_2O)_{172}$. The actual stoichiometry depends on the synthesis conditions since there is usually incomplete filling of the cages by the bromine molecules. No explanation for the wide variety of crystal shapes that can be obtained has been offered.

Dihalogen molecules are often employed as spectroscopic model systems due to their intense optical spectra and the interesting variations in their properties depending on which two halogen atoms are bound together. For instance, since the visible transitions are nominally spin-forbidden, their intensities vary dramatically from F_2 to I_2, even though the identities of the states involved are similar.[8] Also, the symmetry breaking in an interhalogen such as ICl results in selection rules different from those of the homonuclear species. As diatomics with relatively easily assignable orbital symmetries, the halogens serve as model systems for nonlinear optical studies,[9] energy transfer studies,[10,11] and cluster studies.[12,13] Similarly, they are often used to observe how the local environment affects electronic structure, for example, in noble gas matrices,[14] solvents,[15−17] or microporous SiO_2.[18] Given how often halogen molecules are the probe molecule of choice for spectroscopic and dynamics studies, and given that the halogen clathrate hydrates have been known for nearly two centuries, it is quite surprising that there are no published studies of the electronic spectra of halogen clathrate hydrates.

In 1975, Raman spectra for both chlorine and bromine clathrate hydrate were reported, along with that of a BrCl hydrate.[19] The frequencies measured for the Cl_2 and Br_2 stretching vibrations were equal to those of the gas phase, within an experimental error, indicating "little interaction between the guest and the host molecules". The frequency of BrCl was red-shifted by 17 cm^{-1}, presumably due to electrostatic interactions since BrCl has a permanent dipole moment.

Perhaps one reason for the lack of optical spectroscopic data on the halogen clathrate hydrates is that their optical density in a pure crystal is extremely high. To circumvent this issue, we make thin films of polycrystalline bromine clathrate hydrate and

* Corresponding author. E-mail: gkerensk@uci.edu.

10.1021/jp064523q CCC: $33.50
Published on Web 12/10/2006

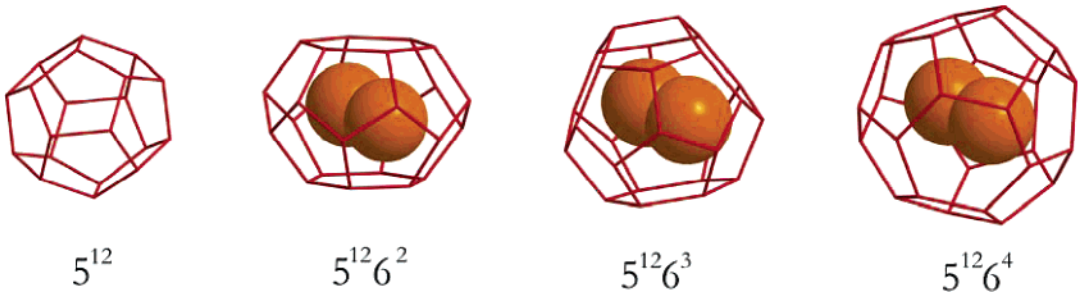

Figure 1. Clathrate hydrate cages of type I and type II and the bromine clathrate hydrate structures. Larger cages are shown with a halogen guest molecule inside.

study them at temperatures where the halogen vapor pressure is negligible. Also, we studied low concentrations of trapped bromine molecules in type II hydrate cages formed with either tetrahydrofuran (THF, C_4H_8O) or methylene chloride (CH_2Cl_2) as the principle hydrate-former guest molecule. Type II hydrates consist of a combination of 5^{12} and $5^{12}6^4$ cages, in a 2:1 ratio. The unit cell is face-centered cubic (space group *Fd*3*m*, $a = 17.3$ Å) with 136 waters and eight guests.[20] The THF or CH_2Cl_2 molecules occupy most of the larger cages, but in this study a small fraction of the large cages is occupied by bromine molecules.

Although no UV−vis spectroscopy has been reported on clathrate hydrate systems, other spectroscopic techniques have been employed. Infrared spectra for ethylene oxide hydrate clathrate were first reported in 1973.[21] Subsequently, Devlin et al. used FTIR spectroscopy to measure the formation kinetics of a variety of hydrate clathrate systems.[22−24] Also, Devlin and Fleyfel reported data in 1988 that show that stretching vibrational frequencies of trapped molecules decrease with increasing cage size and that the size of the small cage of a structure I hydrate increases as the size of the molecules occupying the large cages increases.[25] Sloan et al.[26] monitored the methane Raman transition at 2900 cm^{-1} and its shift and splitting from the value in liquid water, 2911 cm^{-1}, to a pair of values, 2905 and 2915 cm^{-1}, that were assigned to methane in each of the two cages of a type I hydrate. They were also able to use the time dependence of such data to study the rate of hydrate formation as a function of temperature and the presence of an "inhibitor" molecule. Spectra for other molecules have been analyzed with the qualitative "loose cage-tight cage" model of Pimentel and Charles[27], where increases in vibrational frequencies for guest molecules are an indication that they are being constrained by the cage.[28] However, there has been little quantitative analysis of such data. Similarly, NMR spectroscopy often serves as a tool to identify cage occupancy since the resonance frequency is sensitive to the environment and the polarization is a sensitive probe of local anisotropy.[7] NMR also may serve as an important tool to study the kinetics of phase transitions in clathrate hydrates.[29] Given the recent surge in interest in the clathrate hydrates, we can expect a growing number of such studies in the near future.

In the present article, we present optical spectra for bromine trapped in pure clathrate hydrates, in the large cages of type II clathrate hydrates, in solid amorphous ice and in several different solvents. The UV−vis absorption spectra reflect changes in the environment. When bromine is enclathrated in the type II cage, its spectrum is more similar to that of bromine in the gas phase than it is to that of aqueous bromine or bromine in amorphous ice matrix. A qualitative interpretation of these results is presented. Figure 1 shows the four cages of the clathrate hydrates studied here: the usually unfilled by bromine 5^{12} cage, the $5^{12}6^2$ and $5^{12}6^3$ cages that are normally occupied in the bromine clathrate hydrate, and the $5^{12}6^4$ cage that can hold a bromine molecule in either THF or CH_2Cl_2 clathrate hydrate. Although the figures are only schematic, they give an idea of the size ranges of the cages being studied.

Experimental Section

Nanopure distilled water (resistivity greater than 16 MΩ) was used in all experiments. The stated manufactured purity of bromine, tetrahydrofuran (THF, C_4H_8O), cyclohexane (C_6H_{12}), and methylene chloride (CH_2Cl_2) was greater than 99%. No further purification was performed. Absorption measurements in the 190−700 nm spectral range were conducted in a Cary UV−visible spectrometer. For low-temperature scans, the spectrometer was equipped with a glass Dewar with quartz windows and evaporating liquid nitrogen served as the refrigerating fluid. The temperature was monitored by a thermocouple probe.

Absorption spectra of gas-phase Br_2 and Br_2 in solutions were recorded using 10-mm capped quartz cuvettes at $T = 293$K. The samples of bromine in ice were prepared by vapor deposition of the premixed gases, in the ratio 1:500, Br_2-H_2O, on a 0.5-mm sapphire window held at 120 K, as described previously.[9] This flash freezing technique is expected to yield an amorphous arrangement of the water and bromine molecules. Samples of clathrate hydrates were prepared in three different ways:

(1) Polycrystalline samples of bromine hydrate were grown on a surface of a conventional 10 × 10 mm quartz cell from aqueous bromine solutions with Br_2-H_2O ratios ranging from 1:5 to 1:20. The cell was capped to contain the volatile bromine. The crystallization process was initiated on a cell wall by applying dry ice above the mixture level. After bromine and water condensed on the inner surface forming a thin film of a bright orange color, the cell was transferred to a refrigerated bath and maintained at around +3 °C. This temperature is above the melting point of water and bromine, but below that of the bromine clathrate hydrate. This ensures that only solid bromine hydrate is formed. An ideal hydrate film thickness should not exceed 10 μm for absorption measurements due to the high extinction coefficient of Br_2. Usually, times of a few minutes up to an hour of sample conditioning were enough to get sufficient film quality. To avoid contributions to the spectra from gas-phase bromine, the samples were cooled to −20 °C during the measurement. The melting point of solid Br_2 is −7 °C. If solid bromine were to form upon cooling, this would be detected as a strong $Br_2^+-Br_2^-$ charge-transfer absorption band at around 285 nm.[30] Using a similar procedure, we obtained single crystals of bromine hydrate for X-ray analysis. The diffraction pattern obtained was consistent with the previous report of Ripmeester et al.[7]

(2) Polycrystalline samples of bromine-doped THF clathrate hydrate were prepared by cooling near-stoichiometric (C_4H_8O·

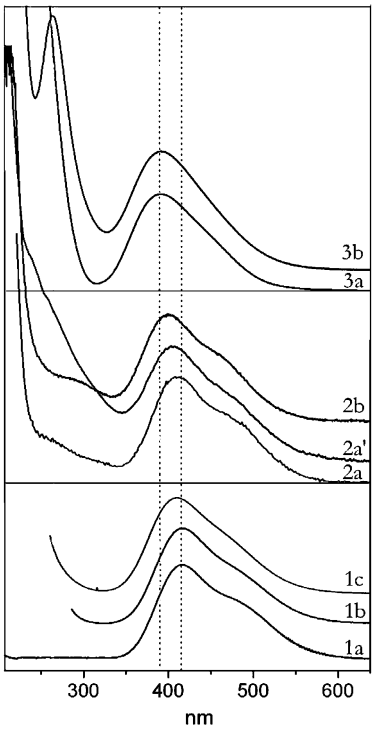

Figure 2. Absorption spectra of Br_2 in: (1a) gas phase (293 K), (1b) C_6H_{12} (293 K), (1c) CH_2Cl_2 (293 K), (2a) $5^{12}6^4$ cages of CH_2Cl_2 type II clathrate hydrate (274 K), (2a′) $5^{12}6^4$ cages of THF type II clathrate hydrate (274 K), (2b) bromine clathrate hydrate (250 K), (3a) amorphous ice (120 K), and (3b) water (293 K). For reference, vertical lines are drawn through the peak of the spectrum of the gas-phase sample and that of the aqueous solution. Note that the peak position for the three clathrate hydrate spectra falls between those of the gas phase and inert solvent spectra of panel 1 and those of the nonclathrate, aqueous spectra of panel 3.

nH_2O, $16 < n < 17$) aqueous THF solutions with a small amount of added Br_2 (less than 10^{-4} Br_2−THF). The lemon-yellow solutions turned more orange-yellow after crystallization. The THF hydrates crystallized easily, and thus the solutions could be cooled directly in the optical cuvettes, forming a reasonably uniform sample. The spectra were recorded between 0 and 4 °C, over which range the samples remained quite clear.

3. Because dichloromethane is not very soluble in water, a more complicated technique was required to form acceptable samples of bromine-doped CH_2Cl_2 clathrate hydrate. Seed crystals were first formed by flash cooling a near-stoichiometric water−CH_2Cl_2 emulsion (with about 10^{-4} Br_2−CH_2Cl_2) at the bottom of a flask. Then, under constant mixing at 0 °C, most of the mixture was converted into an opaque clathrate hydrate ice. A small portion of the sample was pressed between two cooled quartz windows and inserted into the spectrometer. The best temperature range for obtaining good spectra was just above 0 °C.

For each of the clathrate hydrate samples, the melting point corresponded to the literature values: 5.8, 4.4, and 1.7 °C at atmospheric pressure for bromine hydrate, THF hydrate, and CH_2Cl_2 hydrate, respectively.[31]

Results and Analysis

Examples of the spectra obtained in this study are presented in Figure 2, and several properties of the spectra are summarized in Table 1. The data in Figure 2 are divided into three panels. The bottom panel shows spectra of the gas-phase sample and those of bromine in nonaqueous solvents, the top panel shows spectra in liquid water and amorphous ice, and the middle panel shows spectra of bromine in clathrate hydrate cages.

1. Br_2 in the Gas Phase, Nonpolar Solvent, and CH_2Cl_2. Although the gas-phase spectrum of bromine is well-known,[32] we briefly review it here for completeness. The electronic states involved in the valence band spectra are sketched in Figure 3. Three overlapping transitions produce the observed gas-phase absorption band shown in Figure 2.1a. The most intense peak, centered at ~24 000 cm^{-1} (~420 nm), is due to the bound-free $\mathbf{C}^1\Pi_u \leftarrow \mathbf{X}^1\Sigma_g$ transition. The shoulder at ~21 000 cm^{-1} (~480 nm) is due to the $\mathbf{B}^3\Pi_{0u} \leftarrow \mathbf{X}^1\Sigma_g$ transition. Finally, there is a weak tail toward the red due to the $\mathbf{A}^3\Pi_{1u} \leftarrow \mathbf{X}^1\Sigma_g$ transition. In each case, an electron is promoted from the antibonding π^* orbital to the antibonding σ^* orbital. The $\mathbf{B} \leftarrow \mathbf{X}$ and the $\mathbf{A} \leftarrow \mathbf{X}$ transitions are nominally spin-forbidden in the Hund's case (a) coupling scheme and are thus less intense than the $\mathbf{C} \leftarrow \mathbf{X}$ transition. Since Franck−Condon excitation for each transition primarily involves excitation onto the repulsive wall of the excited electronic state, the width of each component is largely defined by the steepness of a repulsive wall. As illustrated in Figure 3, the **C**, **B**, and **A** potential curves are similarly steep in the Franck−Condon region, and therefore, the widths of the three transitions are similar.

The lower panel of Figure 2 shows (1a) a low-resolution spectrum of gas-phase bromine, (1b) bromine in C_6H_{12} solution, and (1c) bromine in CH_2Cl_2 solution, each recorded at room temperature. The spectra are scaled to have approximately the same peak absorbance. Despite their similarity, there are some visible environmental effects. Compared to the gas-phase spectrum, the visible spectrum of Br_2 in a nonpolar cyclohexane shifts to the red by ~100 cm^{-1} and loses contrast between the $\mathbf{C} \leftarrow \mathbf{X}$ and $\mathbf{B} \leftarrow \mathbf{X}$ components. The spectrum in CH_2Cl_2 shifts to the blue[33] by ~450 cm^{-1}, and the band contour smoothens even more, indicating a broadening of the underlying transitions.

In addition to the valence transitions, halogens in solution (even in a nonpolar solution) exhibit strong ultraviolet absorption bands arising from contact charge-transfer interactions with the solvent. These charge-transfer bands are not shown in Figure 2.1 for simplicity.

2. Br_2 in Liquid Water and Amorphous Ice. Compared to the spectra of Br_2 in cyclohexane and CH_2Cl_2, the spectra in liquid water (Figure 2.3b) or amorphous ice (Figure 2.3a) are more strongly shifted and broadened. This can be seen more clearly for comparing the gas-phase spectrum to that of liquid water in Figure 4, for which a cm^{-1} scale is used for the abscissa. In aqueous solution, the valence transitions are centered at around 390 nm, corresponding to a shift of over 1700 cm^{-1}. The additional band at 267 nm is due to the absorption of the tribromide ion.[34,35] The equilibria involved in tribromide ion formation are:

$$Br_2 + H_2O \leftrightarrow HBr + HOBr$$

$$HBr + H_2O \leftrightarrow H_3O^+ + Br^-$$

$$Br_2 + Br^- \leftrightarrow Br_3^-$$

In agreement with the above equilibrium, reducing the bromine concentration of the aqueous solution reduces the relative contribution of the Br_3^- band. The Br_3^- band nests on the wing of a stronger signal assigned to a water−bromine charge-transfer band. Upon freezing, ionic species dissolved in water disappear if equilibrium is maintained. Since the solid samples are formed by flash deposition, and since the charge-

TABLE 1: Parametrization of the Valence Absorption Bands of Br_2 in Different Media

	$\omega_{max}(\mathbf{C}-\mathbf{X})^a$	$\Delta\omega_{max}{}^b$	fwhm^c	$\omega_{max}(\mathbf{B}-\mathbf{X})^a$	$\Delta\omega_{max}{}^b$	fwhm^c
gas	24270	0	3900	20830	0	3650
C_6H_{12}	24160	−120	4000	20760	−70	4000
CCl_4[d]	24390	120	4100	20920	90	4000
CH_2Cl_2	24720	450	4200	21300	470	4100
type II $5^{12}6^4$	24630	360	4000	21190	360	3700
Br_2 hydrate $5^{12}6^2$, $5^{12}6^3$	25150	880	4000	21720	890	3700
amorphous ice, $T = 120$ K	25980	1710	4600	22670	1640	4300
aqueous solution	26000	1730	5000	22590	1760	5000

[a] $\omega_{max}(\mathbf{C},\mathbf{B}-\mathbf{X})$ is the position of the absorption maximum, ±50 cm^{-1}. [b] $\Delta\omega_{max}$ is the shift of the absorption maximum from the gas phase. [c] fwhm $= 2\omega_{max}$ sinh(ln $2/a$) is for the band shape assumed in eq 1, ±10%. [d] Spectrum obtained from the appendix data of ref 36.

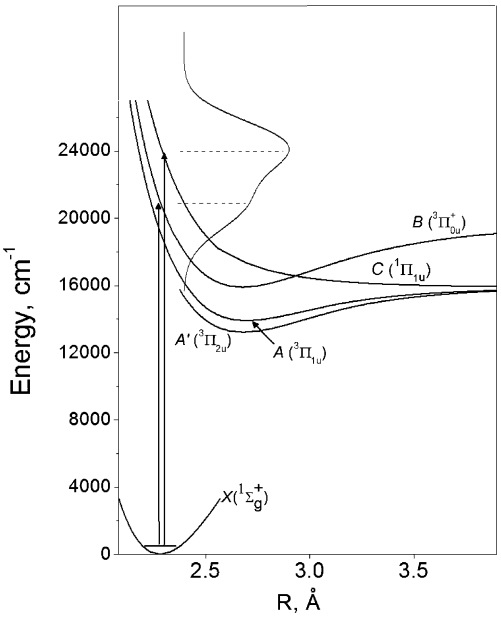

Figure 3. Potential energy curves for five electronic states of Br_2. Vertical arrows mark the **C** ← **X** (24 000 cm^{-1}) and **B** ← **X** (21 000 cm^{-1}) transitions in the visible region. The absorption contour is shown to emphasize the connection between the separation of the potential energy curves and the absorption spectrum.

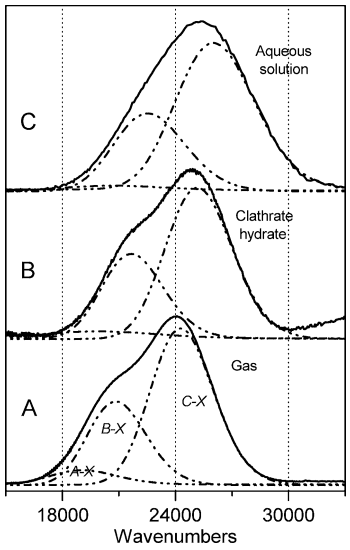

Figure 4. Br_2 absorption spectra in: (A) gas phase (293 K), (B) clathrate hydrate (250 K) (The background signal due to scattered light has been subtracted. The subtraction procedure was guided by a general consideration that in a first approximation the background signal is just an inclined straight line. The resulting uncertainty is included in the error bars.), and (C) liquid water (293 K). The dash-dotted line in each case represents **C** ← **X**, **B** ← **X**, and **A** ← **X** components of the spectra found by nonlinear least-squares fit to the experimental data (see text for details).

transfer band appears to be stronger in the ice sample, it is not clear whether tribromide ions contribute to spectrum 2.3a or whether the entire band in ice should be assigned to charge transfer between guest and host. The main point of interest here is that the valence absorption band of Br_2 in frozen amorphous water ($T = 120$ K) closely resembles that of the aqueous solution. This likeness indicates that the local structure around the bromine and the interactions responsible for the dramatic spectral perturbations have similar origin in both media.

3. Br_2 in Clathrate Hydrate Cages. The spectra of Br_2 confined in clathrate hydrate cages, shown in panel 2 of Figure 2, are more similar to those of Br_2 in the vapor phase than those of Br_2 in liquid water or amorphous ice. Traces 2.2a and 2.2a′ represent the absorption spectra of Br_2 in a type II clathrate hydrate, in large $5^{12}6^4$ cages. As expected, the valence absorption spectra of enclathrated bromine are not sensitive to the identity of the "help" molecule, THF or CH_2Cl_2. In each case, the Br_2 band shifts by only 360 cm^{-1} from the gas phase and its shape changes only slightly. In particular, the underlying **B** ← **X** transition is still discernible at 470 nm. The spectral shift of bromine trapped in the smaller cages of the pure bromine clathrate hydrate, shown in trace 2.2b, is more substantial than those of the type II samples. Still, the band shape retains the characteristic side peak (the **B** ← **X** transition) of the gas-phase spectrum. Thus, the overall appearance of the bromine spectra in the clathrate hydrate cages resembles the gas-phase spectrum more than that of bromine in aqueous solution or solid amorphous ice.

The UV end of the spectra could not be uniquely assigned. Each of the spectra shows increasing absorption to the blue of 350 nm. Since charge-transfer bands have high absorption cross sections, they produce pronounced peaks in the spectra. That of the THF clathrate hydrate sample between 250 and 350 nm is probably due to residual Br_3^- (Figure 2.2a′). The Br_3^- band is much more intense in the THF−water mixture compared to that in pure water, and consequently, minute amounts of these ionic species are detectable in the sample. The strong bands that start to rise at around 240 nm probably belong to charge transfer between Br_2 and the clathrate hydrogen-bonding network since they are similar for each sample. On the other hand, we cannot rule out the possibility that charge transfer between Br_2 and CH_2Cl_2 or THF makes a contribution.

Nonzero baselines result for some bromine hydrate spectra due to Rayleigh scattering. In the spectral decompositions to be described below, this background was subtracted.

4. Decomposition of Br_2 Absorption Band Profiles into C ← X, B ← X, and A ← X Components. The purpose of the present component analysis is to quantify trends of the valence absorptions of Br_2 in various environments. Such component analysis is neither straightforward nor unique as discussed in detail by Tellinghuisen.[32] Structureless spectra are most gainfully

understood in terms of the reflection principle, according to which a band in a spectrum is obtained by reflecting the nuclear probability distribution of the initial ground state onto the difference potential $V_{final} - V_{initial}$.[32] This procedure works well in one dimension, as in the case of diatomics in the gas phase. Unique inversions cannot be expected in the case of multidimensional chromophores. For diatomics in solution, the solute−solvent interactions must be taken into account. Tellinghuisen noted that the absorption spectra of halogens can exhibit significant solvent−solute effects even in inert solvents such as *n*-heptane and CCl_4.[36] Br_2 interacts strongly with water in solution, as evidenced by the large spectral shift and broadening. In a recent analysis,[9] Goldschleger et al. argued that the spectrum cannot be treated as a one-dimensional reflection. Instead, the transition is along both the molecular coordinate and the Br_2–H_2O coordinate, and a two-dimensional reflection is minimally required to obtain a physically meaningful analysis. Here, our intent is to provide a reasonable estimate of the peak positions by a decomposition of the spectra in the three components to be able to highlight the trends as diagnostic of the local environment.

The three overlapping transitions are least squares fitted to a three-parameter lognormal function, which can be regarded as the reflection of a Gaussian distribution from an exponential difference potential:[36]

$$\sigma = \sigma_{max} \exp\{-a[\ln(\omega/\omega_{max})]^2\} \quad (1)$$

where σ_{max} and ω_{max} are amplitude and the position of the absorption maximum, and a is the breadth parameter for each transition. It is not possible to uniquely assign parameters to each transition due to their extensive overlap. Therefore, we have imposed a constraint that the band shifts lie within ± 100 cm^{-1} of that of the dominant **C** ← **X** transition. This assumption is reasonable to the extent that the excited states are similarly perturbed by the environment, as might be expected since they have similar orbital configurations. Taking into account the limitations of the fitting procedure, we assign error bars of ± 50 cm^{-1} to the quoted band shifts of the strongest **C** ← **X** transition upon which our subsequent discussion is based. The **A** ← **X** transitions were included in the fits to account for the red tails of the spectra, but the parameters obtained are not reliable and are not reported or discussed.

Fitting parameters for each of the spectra of Figure 2 are reported in Table 1, and three examples of the resulting decomposition of observed spectra (for the gas phase, the bromine clathrate hydrate, and aqueous solution) are shown in Figure 4. Note the change of scale from nm to cm^{-1}. The fit to the gas-phase Br_2 absorption spectrum at $T = 293$ K yields values that agree with those previously reported by Tellinghuisen.[32]

Note that all band shifts, except those in cyclohexane, are to the blue. Thus, only cyclohexane appears to solvate the Br_2 excited state better than the Br_2 ground state. The trends in nonpolar solvents are more subtle and more difficult to explain, as already noted by Tellinghuisen.[35] In what follows, we focus our discussion on the hydrates, where the spectral perturbations are significantly larger.

Discussion

Consider the strongest **C** ← **X** transition. The band shift is ± 120 cm^{-1} in the two nonpolar solvents, cyclohexane and carbon tetrachloride; 450 cm^{-1} in polar methylene chloride; 360 cm^{-1} inside the relatively large $5^{12}6^4$ cage of a type II clathrate hydrate; 880 cm^{-1} in a combination of the smaller $5^{12}6^2$ and $5^{12}6^3$ cages of the pure bromine clathrate hydrate; and 1730 cm^{-1} in water. Similar trends are obtained for the **B** ← **X** transition.

1. Blue Shift and Broadening of Br_2 Absorption Spectra in Solvents and Amorphous Ice. Our qualitative explanation for the observed blue shift and broadening phenomena in solvents and amorphous ice is based on remarkable results obtained previously for the structures of gas-phase dimers of halogen molecules with noble gas atoms and hydrogen-bonding species, which will be briefly reviewed here. After almost two decades of ambiguous findings and conflicting interpretations, it was discovered that a noble gas atom has almost the same bond energy if it bonds on the end of a halogen molecule to make a linear dimer or perpendicular to the halogen bond to make a "T"-shaped dimer.[37] Perhaps even more surprising is the fact that there is a considerable potential barrier between these two isomers. The noble gas atom feels an extra van der Waals attraction in the "T" conformation since it can interact with both halogen atoms at an optimal distance. This double attraction is balanced by a shorter bond length in the linear conformation, which is important because van der Waals attractive forces scale as $1/r^6$. The shorter bond length in the linear conformation is because the antibonding σ^* orbitals at the ends of the halogen molecules are empty, thereby allowing the noble gas atoms to approach more closely along the halogen bond axis than in other configurations.

This structural difference between the "T"-shaped and linear configurations results in very different spectroscopy and dynamics as first elucidated experimentally for ArI_2[38] and theoretically for $ArCl_2$.[39] These differences are mainly because the excited states obtained by visible laser excitation only have a deep potential well in the "T"-shaped conformation. The linear conformation becomes a saddle point on the excited state because valence electronic excitation moves an electron into the previously empty σ^* orbital. Also, the potential minimum for the Ar−I coordinate for the linear configuration occurs for significantly longer distances than for the T-shaped configuration. Thus, Franck−Condon excitation of the linear ground state leaves the dimer on a repulsive portion of the noble gas−halogen potential. Darr et al.[40] have recently pointed out that what was previously thought of as "the one atom cage effect" is really because a significant fraction of the energy of the incident photon is deposited directly into the noble gas−halogen coordinate and is never available to the halogen−halogen stretching motion. At low resolution, this appears as a substantial blue shift of the halogen absorption spectrum.[39]

The effects described above are even more important for polar molecules bonding to halogen species. This was first observed for the HF−ClF complex.[41] Contrary to expectations, when the hydrogen fluoride molecule, presumably strongly hydrogen bonding, attaches to the polar interhalogen chlorine fluoride, no hydrogen bond is formed. Instead, the lone pairs on the hydrogen fluoride fluorine atom donate electron density to the empty ClF σ^* orbital. Similar to that of the noble gas−halogen species, this bond is unexpectedly short and strong because the empty σ^* orbital on the halogen molecule allows for especially close approach of the lone pair orbital of the HF fluorine atom.

A similar effect was later confirmed for the H_2O−Br_2 dimer, which also forms a linear O−Br−Br configuration with an O−Br bond length of only 2.85 Å.[42] According to ab initio calculations,[42] negligible charge is transferred from water O atom to the bromine molecule upon bond formation. However, the bromine molecule is strongly polarized by the water: 5%

of an electron charge is transferred from the bound Br atom to a free Br atom. Because of this polarization of the bromine molecule, subsequent water molecules add to the bromine end of the core H_2O-Br_2 dimer by hydrogen bonding.[43] The key consideration for the present is the following: although the charge-transfer character of the complex is negligible, charge redistribution accompanies motion along the intermolecular coordinate. As such, the transition dipole is distributed at least along two coordinates: along Br−Br and along Br_2–H_2O. The chromophore in this case is at least two-dimensional.

It is useful to think of two distinct solvent effects on spectra. First, to the extent that the solvent lowers the energy of the ground state more than that of the excited state, the spectrum will be blue-shifted, or, if the effect is reversed, the spectrum will be red-shifted. A different effect is realized when the intermolecular solute−solvent coordinate is quite different in the ground and excited states, as discussed above for ArI_2. In the case of the Br_2–H_2O complex, the solvent coordinate also acquires transition dipole due to charge redistribution. Under the simplifying consideration of separability of coordinates, the spectrum is now the convolution of two one-dimensional spectra, where in each dimension the reflection principle remains valid. Such a treatment was already given to explain the spectra of bromine in water and in amorphous ice.[9] In this picture, the transition leads to direct excitation of the solvent−solute coordinates. In particular, if, as in the present case, a solvent molecule is capable of donating a nonbonding electron pair to the bromine molecule σ^* orbital, a linear configuration is expected for the strongest nearest-neighbor interaction (e.g., O−Br−Br in the case of H_2O-Br_2) and a substantial blue shift and *broadening* of the spectrum is expected because the solvent interaction is strongly bonding in the ground electronic state while a Franck−Condon excitation leaves the excited-state on a repulsive portion of the solvent−solute potential. In this picture, the spectrum of the bromine molecule itself is not significantly shifted, but a significant fraction of the photon energy goes directly into the solvent−solute coordinates.

For the cases considered here, it is unlikely that Br−Br potential changes appreciably upon solvation; most of the changes in the absorption can be attributed to the bromine−solvent interaction. First, with regard to the fact that the two nonpolar solvents shift the valence band in opposite directions, cyclohexane to the red and carbon tetrachloride to the blue, we propose that the difference can be attributed to the chlorine atom lone pairs on the carbon tetrachloride. From the bromine solute molecule's perspective, cyclohexane molecules present mainly a surface of slightly electron-deficient hydrogen atoms. These have no propensity to interact in any particular way with the bromine molecule, and therefore cyclohexane can be considered to be a weakly interacting solvent. Chlorine atoms on the carbon tetrachloride, in contrast to cyclohexane, present a surface of electron lone pairs to the bromine, and one of these lone pairs has a high probability of being in the vicinity of the bromine molecule σ^* orbital. Consequently, this would account for a blue shift of the spectrum.

The effect described in the above paragraph will be even more pronounced for water. In this regard, we note that the dipole moment of water (1.85 D) is only slightly larger than that of methylene chloride (1.6 D), yet the bromine blue shift in water is more than 1700 cm^{-1}, compared to only 450 cm^{-1} in methylene chloride. Clearly, the dipole moment is not the key property for explaining the blue shift. We attribute the large difference to the much higher propensity of the oxygen atom on a water molecule to donate its electrons to the empty bromine σ^* orbital, again requiring that a portion of the photon energy goes directly into the O−Br coordinate upon electronic excitation. The fact that the spectra in aqueous solution and amorphous ice are so similar supports the conclusion that the band position along with the band broadening is determined by short-range interactions.

2. Blue Shift and Minimal Broadening of Br_2 Absorption Spectra in Clathrate Hydrate Cages. We now turn to the spectra of bromine in the clathrate hydrate cages where the absorption bands are blue-shifted but not significantly broadened. In the clathrate hydrate lattice, all of the oxygen lone pairs form hydrogen bonds to other water molecules. Thus, in its most favorable geometry, an encaged bromine molecule can never interact with oxygen lone-pair orbitals. X-ray diffraction measurements[7] at $T = 173$ K show high rotational mobility of Br_2 inside the clathrate cage, implying that there is no preferred orientation. Nondirectional van der Waals forces between the guest and the host are sufficient to stabilize the clathrate hydrate cage. This suggests that the origin of the blue shifts in the clathrate hydrates is quite different than that in water, where the interaction is along the O−Br coordinate, and is most likely due to spatial confinement on the excited electronic states.

The relative cage sizes are illustrated in Figure 1. In the case of the type II $5^{12}6^4$ cage, the estimated cage diameter, 6.6 Å,[44] is appreciably larger than the bromine ground state van der Waals length, 5.7 Å.[45] Indeed, the observed absorption shift is only 360 cm^{-1}. For the pure bromine clathrate hydrate, the bromine is in a combination of $5^{12}6^2$ and $5^{12}6^3$ cages. Since there are four $5^{12}6^2$ cages for every $5^{12}6^3$ cage, the spectrum is probably dominated by the smaller cage size, with an effective cage diameter of 5.86 Å. In the excited B-state, the Br_2 bond expands by 0.4 Å and is unbound in the C-state, and the excited states are confined by the cage. The resulting blue shift is 880 cm^{-1}. Even for such a pronounced shift, the widths of both bands in the clathrate hydrate spectra remain practically identical to those in the gas phase, indicating that the transition dipole remains along the molecular coordinate. This supports our interpretation that the inside of a clathrate hydrate cage is a nearly isotropic van der Waals sphere as far as the bromine molecules are concerned. Although the above discussion concentrates on interpreting the shifts in the **C** ← **X** bands in the bromine spectra, we note here that the values obtained for the **B** ← **X** bands are quite similar to those for the **C** ← **X** bands. This is satisfying since the orbital occupancies of the **B** and **C** states are similar.

The interpretation we have presented in this article is speculative. However, the results, especially the differences between the bromine spectra in the type II cages compared to those in aqueous solution, are so dramatic that such a qualitative interpretation is justified. Similarly, the differences between the spectra in the two nonpolar solvents illustrate that any useful interpretation must take into account the local environment around the bromine. Theoretical work on model systems would be extremely valuable to judge the validity of the model presented here.

Conclusion

We have reported the first optical spectroscopic study of bromine molecules trapped into clathrate hydrate cages, along with data for bromine spectra in nonpolar and polar solvents, in aqueous solution, and in amorphous ice. The band maxima and the bandwidths for the bromine valence transitions are quite sensitive to the local environment. We present a qualitative model that is based on the fact that electron donation from the

nearest-neighbor solvent molecule into the bromine ground-state σ^* orbital is crucial for understanding the spectra. To the extent that this occurs, Franck−Condon electronic excitation necessarily deposits considerable energy into the nearest-neighbor solvent−Br coordinate. Indeed, the band shift and width in liquid-phase spectra scale, at least qualitatively, with the propensity of the solvent molecule to donate electron pairs. The visible spectra of the halogen molecules in the clathrate hydrate cages are more similar to those of the gas phase than to those of bromine in liquid water or amorphous ice because all of the oxygen lone pair electrons in the clathrate hydrate cages are included in hydrogen bonds and are thus unavailable for donation to the bromine molecules. The shift of the absorption spectra in this case might be explained by the spatial constraints imposed by the cage walls.

Acknowledgment. This work was supported by the U.S. National Science Foundation Grant No. CHE-0404743. We thank John Kenny, Evan Neidholdt, Kimberly Gock, Annie Pham, Meghan Krege, Joanne Abbondondola, and Robert Ferazzi for their suggestions and assistance in preparing optical quality samples for this study.

References and Notes

(1) Davy, H. *Philos. Trans. R. Soc. London* **1811**, *101*, 155.
(2) Lowig, C. *Ann. Chim. Phys.* **1829**, *42*, 1829.
(3) Pauling, L.; Marsh, R. E. *Proc. Natl. Acad. Sci. U.S.A.* **1952**, *38*, 112.
(4) Cady, G. H. *J. Phys. Chem.* **1981**, *85*, 3225.
(5) Allen, K. W.; Jeffrey, G. A. *J. Chem. Phys.* **1963**, *38*, 2304.
(6) Dyadin, Y. A.; Belosludov, V. R. *Compr. Supramol. Chem.* **1996**, *6*, 789.
(7) Udachin, K. A.; Enright, G. D.; Ratcliffe, C. I.; Ripmeester, J. A. *J. Am. Chem. Soc.* **1997**, *119*, 11481.
(8) Heaven, M. C. *Chem. Soc. Rev.* **1986**, *15*, 405.
(9) Goldschleger, I. U.; Senekerimyan, V.; Krage, M. S.; Seferyan, H.; Janda, K. C.; Apkarian, V. A. *J. Chem. Phys.* **2006**, *124*, 204507/1.
(10) Steinfeld, J. I.; Klemperer, W. *J. Chem. Phys.* **1965**, *42*, 3475.
(11) Krajnovich, D. J.; Butz, K. W.; Du, H.; Parmenter, C. S. *J. Chem. Phys.* **1989**, *91*, 7725.
(12) Heaven, M. C. *J. Phys. Chem.* **1993**, *97*, 8567.
(13) Rohrbacher, A.; Halberstadt, N.; Janda, K. C. *Annu. Rev. Phys. Chem.* **2000**, *51*, 405.
(14) Bondybey, V. E.; Bearder, S. S.; Fletcher, C. *J. Chem. Phys.* **1976**, *64*, 5243.
(15) Aickin, R. G.; Bayliss, N. S.; Rees, A. L. G. *Proc. R. Soc. London* **1938**, *A169*, 234.
(16) Child, C. L.; Walker, O. J. *Trans. Faraday Soc.* **1938**, *34*, 1506.
(17) Geilhaupt, M.; Dorfmueller, T. *Chem. Phys.* **1983**, *76*, 443.
(18) Wirnsberger, G.; Fritzer, H. P.; Popitsch, A.; van de Goor, G.; Behrens, P. *Angew. Chem., Int. Ed.* **1997**, *35*, 2777.
(19) Anthonsen, J. W. *Acta Chem. Scand., Ser. A* **1975**, *29*, 175.
(20) Jeffrey, G. A. *An Introduction to Hydrogen Bonding*; Oxford University Press: New York, 1997.
(21) Bertie, J. E.; Othen, D. A. *Can. J. Chem.* **1973**, *51*, 1159.
(22) Bertie, J. E.; Devlin, J. P. *J. Chem. Phys.* **1983**, *78*, 6340.
(23) Richardson, H. H.; Wooldridge, P. J.; Devlin, J. P. *J. Phys. Chem.* **1985**, *89*, 3552.
(24) Gulluru, D. B.; Devlin, J. P. *J. Phys. Chem. A.* **2006**, *110*, 1901.
(25) Fleyfel, F.; Devlin, J. P. *J. Phys. Chem.* **1988**, *92*, 631.
(26) Sloan, E. D.; Subramanian, S.; Matthews, P. N.; Lederhos, J. P.; Khokhar, A. A. *Ind. Eng. Chem. Res.* **1998**, *37*, 3124.
(27) Pimentel, G. C.; Charles, S. W. *Pure Appl. Chem.* **1963**, *7*, 111.
(28) Subramanian, S.; Sloan, J. E. D. *J. Phys. Chem. B* **2002**, *106*, 4348.
(29) Gao, S.; House, W.; Chapman, W. G. *J. Phys. Chem. B* **2005**, *109*, 19090.
(30) Krage, M. S. The photophysics of solid bromine: a study of chain reaction mediated electronic relaxation. University of California, Irvine, CA, 2006.
(31) Davidson, D. W. *Water, A Comprehensive Treatise*; Plenum: New York, 1973; Vol. 2, pp 115−234.
(32) Tellinghuisen, J. *J. Chem. Phys.* **2001**, *115*, 10417.
(33) Since absorption of bromine in all considered media (except for Br_2 in C_6H_{12}) shifts to the blue, we will further refer only to the shift magnitude and not the direction.
(34) Katzin, L. I. *J. Chem. Phys.* **1955**, *23*, 2055.
(35) Milne, J. *Spectrochim. Acta., Part A* **1992**, *48*, 533.
(36) Gray, R. I.; Luckett, K. M.; Tellinghuisen, J. *J. Phys. Chem. A* **2001**, *105*, 11183.
(37) Rohrbacher, A.; Williams, J.; Janda, K. C. *Phys. Chem. Chem. Phys.* **1999**, *1*, 5263.
(38) Burke, M. L.; Klemperer, W. *J. Chem. Phys.* **1993**, *98*, 1797.
(39) Janda, K. C.; Djahanddideh, D.; Roncero, O.; Halberstadt, N. *Chem. Phys.* **1998**, *239*.
(40) Darr, J. P.; Glennon, J. J.; Loomis, R. A. *J. Chem. Phys.* **2005**, *122*, 131101.
(41) Novick, S. E.; Janda, K. C.; Klemperer, W. *J. Chem. Phys.* **1976**, *65*, 5115.
(42) Legon, A. C.; Thumwood, J. M. A.; Waclawik, E. R. *Chem.−Eur. J.* **2002**, *8*, 940.
(43) Ramondo, F.; Sodeau, J. R.; Roddis, T. B.; Williams, N. A. *Phys. Chem. Chem. Phys.* **2000**, *2*, 2309.
(44) This value is obtained by subtracting the water van der Waals diameter from the cage diameter.
(45) This is the bond length plus the atomic van der Waals diameter.